Separation Science and Technology
Publication details, including instructions for authors and subscription information:
http://www.informaworld.com/smpp/title~content=t713708471

Numerical Simulation of Concentration Polarization in a Pervaporation Module

Ming Peng[a]; Leland M. Vane[b]; Sean X. Liu[a]
[a] Department of Food Science, Rutgers University, New Brunswick, New Jersey, USA [b] National Risk Management Research Laboratory, U.S. Environmental Protection Agency, Cincinnati, Ohio, USA

Online publication date: 08 July 2010

To cite this Article Peng, Ming , Vane, Leland M. and Liu, Sean X.(2005) 'Numerical Simulation of Concentration Polarization in a Pervaporation Module', Separation Science and Technology, 39: 6, 1239 — 1257
To link to this Article: DOI: 10.1081/SS-120030480
URL: http://dx.doi.org/10.1081/SS-120030480

SEPARATION SCIENCE AND TECHNOLOGY
Vol. 39, No. 6, pp. 1239–1257, 2004

Numerical Simulation of Concentration Polarization in a Pervaporation Module

Ming Peng,[1] Leland M. Vane,[2] and Sean X. Liu[1,*]

[1]Department of Food Science, Rutgers University, New Brunswick, New Jersey, USA
[2]National Risk Management Research Laboratory, U.S. Environmental Protection Agency, Cincinnati, Ohio, USA

ABSTRACT

A mathematical model was developed to describe mass transfer in a slit flow channel formed by a thin supported membrane at the bottom and an impermeable stainless steel block at the top in a lab-scale flat sheet pervaporation membrane module. Boundary layer theory was employed to obtain the mass transfer equations governing mass transport in the liquid boundary layer and in the membrane matrix. Equations of the model were solved numerically with computational fluid dynamics (CFD) techniques.

*Correspondence: Sean X. Liu, Department of Food Science, Rutgers University, 65 Dudley Road, New Brunswick, NJ 08901, USA; Fax: (732) 932-6776; E-mail: liu@aesop.rutgers.edu.

DOI: 10.1081/SS-120030480 0149-6395 (Print); 1520-5754 (Online)

The extent of concentration polarization and its impact upon permeation flux rate under different conditions were examined.

Key Words: Mass transfer coefficient; Model; Pervaporation; Concentration polarization; CFD.

INTRODUCTION

Pervaporation (PV) is a membrane separation process that can be used for separating trace amount of volatile compound(s) from a bulk feed solution.[1] Research in the last two decades has shown that this is a promising technology in separating azeotropic mixtures,[2] removing volatile organic compounds (VOCs) from contaminated groundwater,[3–6] or recovering aroma flavor compounds during food and beverage manufacturing processes.[7] In this process, one side of a non-porous membrane is exposed to a liquid feed stream and a vacuum or sweep gas is applied to the downstream side of the membrane (permeate). The component or components targeted for removal permeate the membrane and evaporate into the permeate stream. The reduced partial pressure of compounds in permeate provides the driving force for the separation. The slowly permeating components remain in the retentate and can be considered purified.

Accurate depiction of mass transfer phenomena during a PV process is a critical issue for successful evaluation and application of this emerging technology. The driving force for mass transport of permeating species is the partial vapor pressure difference between two sides of the non-porous pervaporation membrane. As pervaporative mass transfer takes place across the membrane, the concentration(s) of the preferentially permeated component(s) at the upstream membrane surface could be much lower than those in the bulk phase if the rate of mass transport of the permeating species from the bulk to the membrane surface is slower than that through the membrane. This phenomenon is known as concentration polarization. As noted by several researchers, concentration polarization is determined by membrane permeability, hydrodynamic conditions, and membrane selectivity.[8–10] By combining mass transport processes in different stages with a total material balance, the extent to which the actual permeation flux is reduced as compared to the flux in an idealized situation, i.e., no mass transfer resistance in the boundary layer near the membrane, can be estimated. However, this approach cannot be used to predict permeation flux for a PV module and membrane for which no empirical data exists, as neither flux nor reduced concentration at the upstream membrane surface can be determined beforehand.

MARCEL DEKKER, INC.
270 Madison Avenue, New York, New York 10016

Dimensionless correlation was sometimes used for calculating mass transfer coefficient in the concentration boundary layer near the membrane surface. By making an analogy to heat transfer, empirical heat transfer equations were adopted for calculating mass transfer coefficients in concentration boundary layers.[3,7,11] The difficulty in this approach is that available empirical equations could not take into account different PV module geometries and that assumptions made in the correlations might not always be satisfactory. As flow dynamics vary with structural and geometrical characteristics within the modules, it is not possible to have a universal empirical equation for all pervaporative mass transfer situations.

The objective of this study was to propose a numerical model that incorporated analysis of fluid dynamics as well as mass transfer occurring at the membrane boundary layer in a flat sheet PV module, and to examine the role of the concentration boundary layer in mass transfer processes. A commercial computational fluid dynamics (CFD) package, FLUENT® 6.0 with GAMBIT® 2.0, was used in hydrodynamics mappings and mass transfer computations. GAMBIT® 2.0 provides complete meshing flexibility in solving flow problems with structured meshes. FLUENT® is a computer program for modeling fluid flow and heat transfer. All functions required to compute a solution and to display the results in the FLUENT® software were accessible either through an interactive interface or by constructing user-defined-functions (UDS).

THEORETICAL CONSIDERATIONS FOR MODELING MASS TRANSFER IN THE LIQUID BOUNDARY LAYER

Mass Transport of Permeating Component in a Pervaporation Process

The physicochemical aspects of a pervaporation process are generally described as a solution-diffusion model[7] that consists of five consecutive steps as target compound(s) diffuse through the liquid boundary layer next to the feed side of the membrane (step 1), followed by selective partitioning (step 2) into and diffusion (step 3) through membrane, and finalized by desorption (step 4) from membrane and diffusion (step 5) through the vapor phase on the permeate side. For convenience, VOC removal from water will be used as an example for the following discussion. The slowest step in this sequence will limit the overall rate of mass transfer and will be the center of research focus. The partitioning and desorption steps are generally not considered to be rate limiting. Indeed it is usually assumed that an almost equilibrium condition prevails at the interface between the membrane and the fluid phases,

MARCEL DEKKER, INC.
270 Madison Avenue, New York, New York 10016

therefore, one or more of steps 1, 3, 5 may control the rate of mass transfer. These steps are conveniently expressed with mathematical symbols as:

$$\frac{1}{k^{ov}} = \frac{1}{k^{bl}} + \frac{1}{k^{m}} + \frac{1}{k^{v}} \tag{1}$$

The ks (m/sec) appearing in the equation are mass transfer coefficients, and their reciprocals represent the mass transfer resistance at each step. Superscripts, ov, bl, m, and v denote overall, liquid boundary layer, membrane, and vapor phase boundary layer, respectively. For many pervaporation processes, a strong vacuum (i.e., less than 100 torr absolute pressure) is applied at the permeate side and, therefore, the mass transfer resistance in the vapor boundary layer is negligible. This leaves only the liquid boundary layer ($1/k^{bl}$) and membrane ($1/k^{m}$) resistances in Eq. (1).

The effect of mass transfer resistance in the boundary layer on pervaporation performance has been attracting attention from the scientific community since the early inception of pervaporation technology. One common approach to address the mass transfer resistance in the liquid boundary layer is to establish a Sherwood correlation among process parameters evaluated from the experimental data. The most widely used modified Sherwood correlation for pervaporation analysis is Leveque's equation based on film theory and derived from heat transfer analog for a developing flow in an open conduit:

$$k = 1.6\left(\frac{UD^2}{d_h L}\right)^{1/3} \tag{2}$$

where D (m^2/sec) is the diffusivity of the solute in the solution, d_h (m), the hydraulic diameter of the flow path; L (m), the length of pathway of the retentate in a cross-flow mode; and U (m/sec) is the mean feed solution velocity. As will be shown in "Results and Discussions," the use of this correlation might not predict accurately the mass transfer coefficient in the boundary layer.

Module Geometry and the Governing Equations

The PV module simulated in this research was a bench-scale flat sheet module as shown in a schematic diagram in Fig. 1. In this slit-type module, the membrane is located at the bottom of the slit while the top or "roof" of the slit is impermeable. This type of module allows easy evaluation of the performance of different PV membrane. The velocities were assumed to reach steady parabolic profiles shortly after entering module slit where the membrane is situated. Similarly, concentration in the slit would form a gradient

Marcel Dekker, Inc.
270 Madison Avenue, New York, New York 10016

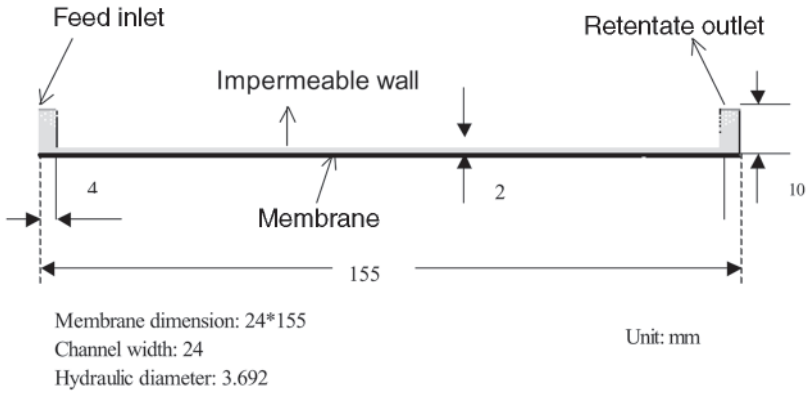

Figure 1. A schematic illustration of the pervaporation membrane flow channel.

near the surface of the membrane. Due to the small magnitude of permeation velocities of the VOC in y-direction (perpendicular to the membrane surface), it is reasonable to assume that permeation velocities have no effect on overall velocity profile within the slit.

Governing equations based on the equation of overall mass conservation, the equations of momentum conservation and the equation of mass conservation for the solute (VOC) are as follows.

Continuity equation

$$\frac{\partial u}{\partial x}+\frac{\partial v}{\partial y}=0 \tag{3}$$

Momentum conservation: in x-direction

$$u\frac{\partial u}{\partial x}+v\frac{\partial u}{\partial y}=-\frac{1}{\rho}\frac{\partial p}{\partial x}+\frac{\mu}{\rho}\left(\frac{\partial^2 u}{\partial x^2}+\frac{\partial^2 u}{\partial y^2}\right) \tag{4}$$

in y-direction

$$u\frac{\partial v}{\partial x}+v\frac{\partial v}{\partial y}=-\frac{1}{\rho}\frac{\partial p}{\partial x}+\frac{\mu}{\rho}\left(\frac{\partial^2 v}{\partial x^2}+\frac{\partial^2 v}{\partial y^2}\right) \tag{5}$$

Mass conservation for VOC:

$$u\frac{\partial c}{\partial x}+v\frac{\partial c}{\partial y}=D\left(\frac{\partial^2 c}{\partial x^2}+\frac{\partial^2 c}{\partial y^2}\right) \tag{6}$$

Marcel Dekker, Inc.
270 Madison Avenue, New York, New York 10016

In the above equations, u and v are velocities in x and y direction, respectively, within the membrane channel; p is pressure; ρ is fluid density; μ is fluid viscosity; D is the diffusion coefficient for VOC in an aqueous solution.

Assumptions and Boundary Conditions

The preliminary assumptions used for solving equations included: (1) steady state operation; (2) laminar flow regime; (3) non-slip boundary conditions at wall surfaces; (4) partitioning of the target compound from the bulk feed solution into the membrane is fast (i.e., not mass transfer limiting); and (5) negligible membrane resistance. One additional assumption is that VOC content in feed stream is low so that there is no or negligible membrane swelling. For some organophilic pervaporation such as organic solvent concentration, membrane swelling could be substantial, which will influence mass transfer within membrane matrix. This is not considered in this study. Assuming negligible membrane resistance would lead to a mass transfer coefficient in boundary layer under idealized situation, i.e., total mass transfer resistance comes from boundary layer. By this assumption, target solute(s) would be able to diffuse fast enough from the membrane surface into downside vapor side; therefore, mass transfer at the membrane surface could be taken as a pseudo-chemical reaction happening on the membrane surface. This can be expressed as a first-order reaction, which is consistent with the principle of Henry's law.

$$\text{VOC\_in\_solution} \longrightarrow \text{VOC\_in\_membrane}$$

The Henry's law constant for the target compound partitioning between water and the membrane phases describes the equilibrium state, i.e., the concentration in the membrane varies linearly with VOC concentration in water where the solution is dilute. In essence, the introduction of reaction constant k will help to define the overall effects of all boundary conditions starting from the membrane to the permeate (vapor) side.

$$\frac{d[\text{VOC\_in\_water}]}{dt} = -\frac{d[\text{VOC\_in\_membrane}]}{dt} \tag{7}$$

$$\frac{d[\text{VOC\_in\_water}]}{dt} = -kS[\text{VOC\_in\_water}](\text{g/sec}) \tag{8}$$

The right term in Eq. (8) is the trans-membrane flow rate of permeate. The time derivative in above equations indicate that for a batch PV operation the whole process will be an unsteady process, i.e., permeate of organic compound through membrane will cause a concentration decrease in feed tank.

MARCEL DEKKER, INC.
270 Madison Avenue, New York, New York 10016

When PV is carried out in continuous steady state with constant feed concentration, a balance will be established between diffusion of organic compounds with the amount expressed by chemical reaction mechanism. This approach takes analogy to kinetics of heterogeneous process in literature[14] where a mass delivery coefficient was used to describe kinetics of a dissolving process.

The reaction rate constant observes the Arrhenius relationship:

$$k = A \exp\left(-\frac{E_a}{RT}\right) \tag{9}$$

where E_a is the reaction activation energy (kJ/kmol), R is universal gas constant, T is absolute temperature (K).

When this reaction rate constant decreases, it will correspond to a certain increase in the membrane resistance. The concentration profile near the membrane surface and permeation flux corresponding to different membrane resistance could, therefore, be predicted. As PV separation is mostly used in separating compounds from dilute solutions, water flux is usually relatively constant and not subject to concentration polarization. Its flux can be either treated by a similar Arrhenius equation or by using available experiment data.

Numerical Simulation of the Model

The meshing work for the geometry of PV bench unit was done with GAMBIT® 2.0. Altogether 11,2003 nodes representing 10,8700 cells were used for meshing height (0.002 m) and length (0.155 m) in 2-D analyses. Grid refinement was performed according to concentration gradient within module geometry. The final result represented the result after completing grid refinement and grid independence. The width was taken as infinite. The criteria for convergence are 1.2×10^{-6} for continuity, 1×10^{-7} for velocity, 1×10^{-8} for the organic compound (solute concentration). FLUENT® predefined macros were used for calculations of concentration boundary layer thickness that was arbitrarily defined as a thin layer of solution with the concentration of which falls below 99% of the VOC concentration in the feed stream. The parameters used for the simulation are shown in Table 1.

RESULTS AND DISCUSSIONS

The numerical calculations produced much more information regarding mass transfer in the boundary layer than a typical empirical correlation. As shown below, the concentration boundary layer is a developing layer

MARCEL DEKKER, INC.
270 Madison Avenue, New York, New York 10016

Table 1. Parameters used for numerical simulations.

Operating parameters	Variation range
Feed concentration	50–600 mg/L
Feed flow rate	0.0063–0.018 L/sec
Temperature	30°C
Permeate pressure	Kept at 2–3 torr
Diffusion coefficient of VOC at 30°C	1.1×10^{-9} m^2 sec[a]
Feed stream density	1,000 kg/m^3
Feed viscosity at 30°C	0.00086 kg/m sec
E_a	45,000 kJ/kmol

[a]Calculated by Wilke–Chang equation.

along the membrane surface rather than a stagnant layer as prescribed by the film theory. The velocity profile, concentration profile near membrane surface, local flux as a function of position along pathway on membrane, and inlet effect on the concentration boundary layer are also described below.

Velocity Profile

Velocity profiles are important for interpreting concentration and flux profiles. The velocity profile in the module is shown in Fig. 2. The mass average velocity shown was 0.1 m/sec, corresponding to Reynolds number (*Re*) of 450. It is apparent from Fig. 2 that the maximum velocity of 0.15 m/sec occurs in the middle of the height of the module slit. This result was in agreement with the analytical solution in the literature,[13] i.e., maximum velocity of laminar flow in a narrow slit is 1.5 times the average velocity.

Figures 3 and 4 show the velocity contour and velocity vector near the inlet of the module. It was indicated that the velocity reached fully developed profile quickly. An apparent inlet effect was present in light of reduced velocity boundary layer near the inlet, which had strong effect on local solute permeation flux. Also a stagnant zone was present near the corner of the module. The flux profile was influenced by the hydrodynamic (velocity) profile.

Flux Profile and Effects of Feed Concentration and Velocity on Flux

As preferential permeation through the membrane always results in a concentration of solute lower than that in the bulk feed solution in a PV operation,

Marcel Dekker, Inc.
270 Madison Avenue, New York, New York 10016

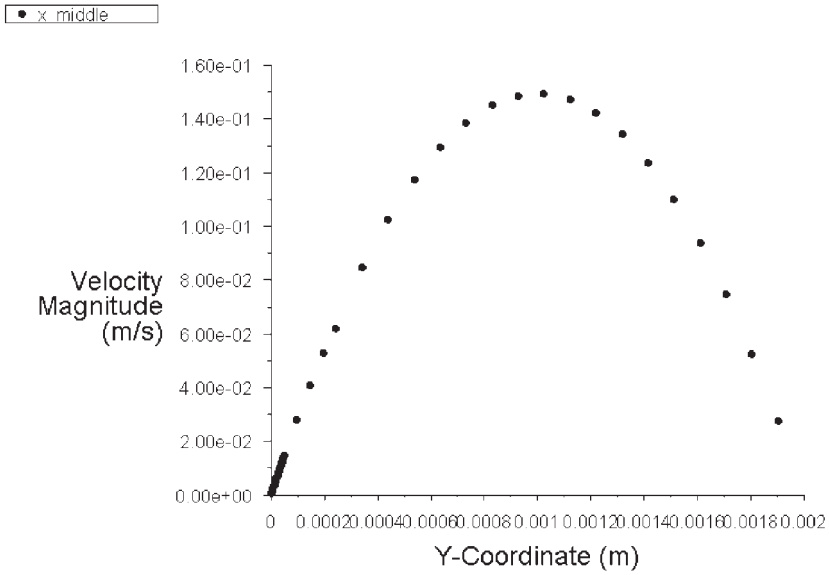

Figure 2. Velocity profile within membrane module, mass average velocity at slit above the membrane surface was 0.1 m/sec.

the solute flux is therefore regulated by both feed concentration and flow regime. With the assumption of negligible membrane resistance, the maximum flux could be calculated as shown in Fig. 5, which described the local flux along the membrane surface for different incoming feed concentrations. Though feed stream solution influenced local flux value, the flux profiles were the same. Over much of the membrane area the flux showed a slight decreasing trend, indicating increased concentration polarization severity. A peak in flux is predicted near the module inlet. By examining velocity vectors at the inlet of the module channel, the feed stream was found to accelerate immediately after the inlet, which lowered the velocity boundary layer thickness and increased mass transport efficiency. Before that peak, there is an almost stagnant corner, which explains the very low flux at the very beginning of the membrane channel. At the outlet, there is both a thin stagnant zone and a vortex zone, which resulted a steeper decreasing trend of flux near the outlet.

The driving force of PV operation is chemical potential difference between two sides of the membrane. On the vacuum side the concentration of VOC is very low because of high degree of vacuum. As a consequence, the increase in feed concentration will increase the driving force for the pervaporation process, thus increasing the flux of VOC permeation. The area-averaged fluxes

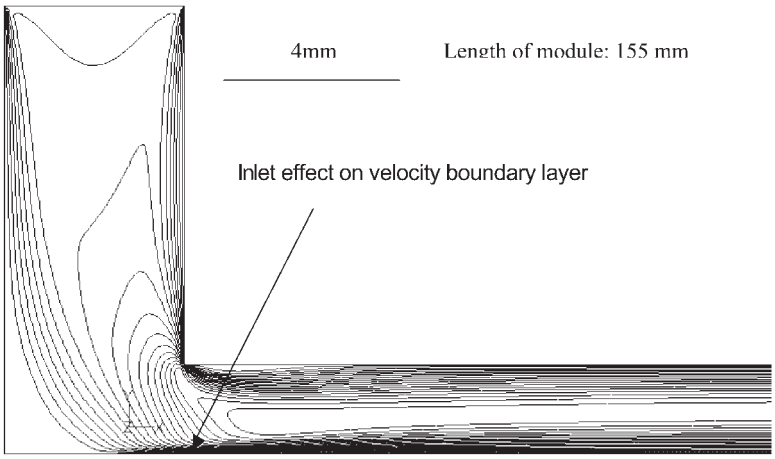

Figure 3. Velocity contour at the membrane inlet.

of VOC at feed concentrations of 300 and 600 ppm in Fig. 5 were found to be 3.29×10^{-6} and 6.58×10^{-6} kg/m^2 sec, equivalent to 11.8 and 23.7 g/m^2 hr. Thus, a linear relationship between VOC flux and feed concentration was observed.

When membrane resistance was neglected, the increase of velocity in laminar regime always brought a decrease in boundary layer thickness and an increase in flux. The extent of the boundary layer was registered by examining the grid coordinates of the cells where concentrations were 99% of the

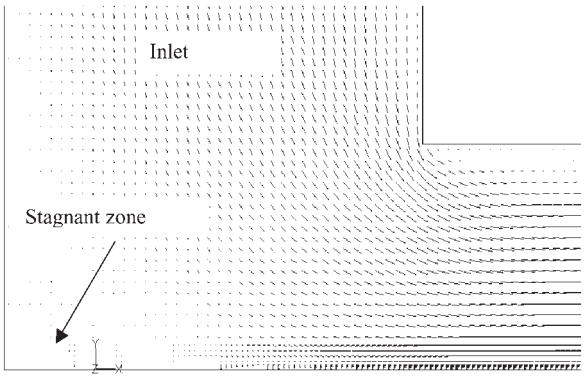

Figure 4. Velocity vectors at the inlet of PV module.

MARCEL DEKKER, INC.
270 Madison Avenue, New York, New York 10016

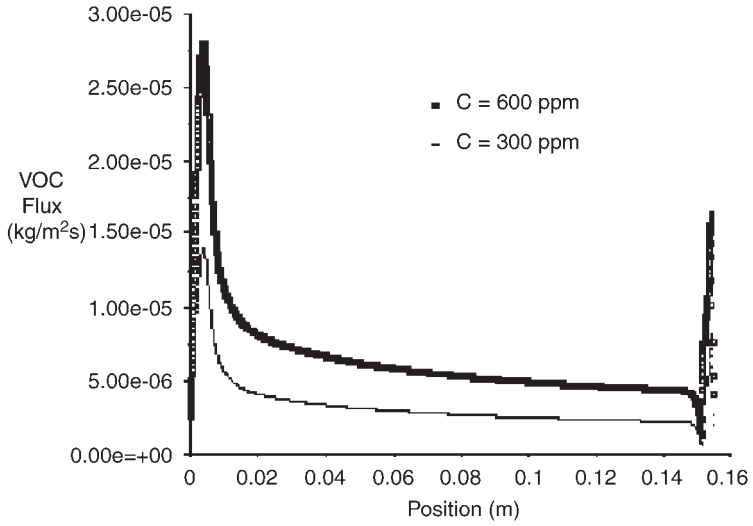

Figure 5. VOC flux at two different feed concentrations of 300 and 600 ppm (top data set) as a function of distance (x) from the feed inlet. Average velocity at the inlet is 0.05 m/sec, corresponding to *Re* of 450. The values for high points at the right corner of the diagram showed the effect of turbulence mixing at the outlet. These values will not be included in calculating average flux.

original feed concentration. Figure 6 shows that at a low *Re* of 450, the maximum concentration boundary layer thickness reached 12.5% of the height of the membrane channel (0.25 mm) compared to 8.75% (0.17 mm) when *Re* is 1800 (the average incoming velocity at the inlet is 0.2 m/sec). The fluxes under these two velocities are shown in Fig. 7. The area-averaged flux at *Re* of 1800 was found to be 5.54×10^{-6} kg/m^2 sec, equivalent to 19.9 g/m^2 hr, which showed about 68% increase over flow regime when *Re* was 450 (Table 2).

It can be observed that the adverse effect of concentration polarization became more serious near the outlet of the module. Any measures of reducing concentration polarization in this region would be significant in terms of improving PV performance.

Membrane Resistance

Despite much progress in membrane material development and the availability of asymmetric membrane where very thin layer (around 3 μm)

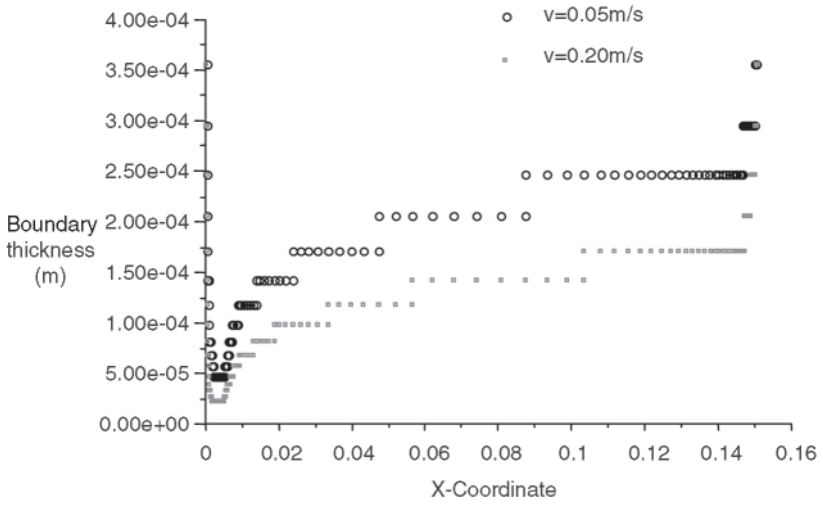

Figure 6. The values of concentration boundary layer thickness at *Re* 450 and 1800.

of active separation membrane supported by a porous media, the membrane resistance is not always negligible. When membrane resistance contributes significantly to overall mass transfer resistance, the idealized flux in previous discussion could not be achieved. In this circumstance, adjustment of the reaction constant at the membrane surface, which corresponds to the increased membrane resistance, is needed. As a result of that, surface concentrations would increase due to the less efficient membrane performance. The overall effect is that flux will decrease based on the magnitude of membrane resistance.

In order to simulate varying membrane resistance, different reaction rate constants within a reasonable range of $0.01-10^{-6}$ were set as boundary condition for calculation. The upper extreme represents a point over which the flux will show no increase, indicating membrane resistance is much smaller (about one thousandth) as compared to resistance from concentration boundary layer. The lower extreme represents a point that membrane resistance is of substantial proportion (about 90%) of overall resistance. The correlation between reaction rate constant and membrane resistance was established by practices in the following sequence: firstly set a specific rate constant and carried out iterations until convergence criteria were satisfied; secondly extracted data for area-averaged overall flux and area-averaged concentration in aqueous phase near membrane surface according to concentration profile; then overall resistance and resistance from concentration boundary layer can be

MARCEL DEKKER, INC.
270 Madison Avenue, New York, New York 10016

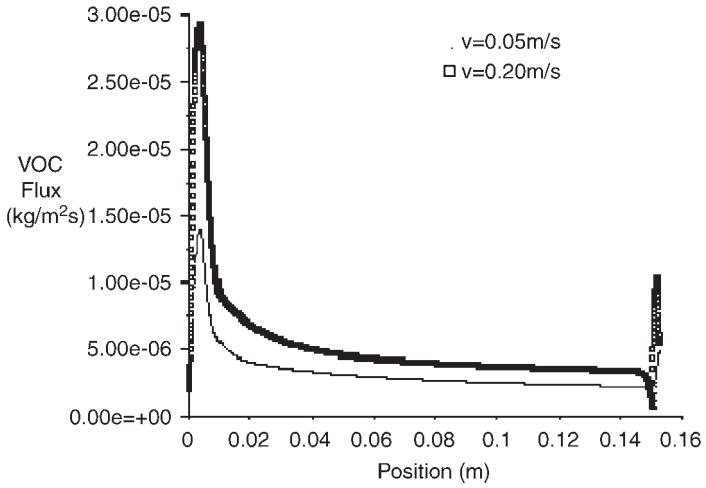

Figure 7. VOC flux at average inlet velocities of 0.2 and 0.05 m/sec, where feed concentration was 300 ppm. The corresponding Reynolds numbers parallel to the membrane surface were 1800 and 450, respectively.

calculated, the difference of these two resistance is the resistance coming from membrane in this specific setting under steady state. After repeating calculations, the flux, overall resistance, local concentration profile, and membrane resistance corresponding to different extent of separation efficiency can be obtained.

Figure 8 shows the calculated membrane resistance that corresponds to a reaction rate setting under the flow regime of $Re = 450$. The relative surface concentration, defined as the ratio of average surface concentration to bulk feed solution, increased exponentially with the increase of membrane resistance.

Table 2. Average VOC flux and mass transfer coefficient in the boundary layer.

Re	Average flux (g/m^2 hr)	Mass transfer coefficient (m/sec) $\times 10^5$
450	11.8	1.10
900	15.6	1.44
1,800	19.9	1.85

Note: Feed concentration 300 ppm, diffusivity 1.1×10^{-9}, $T = 30^{\circ}C$.

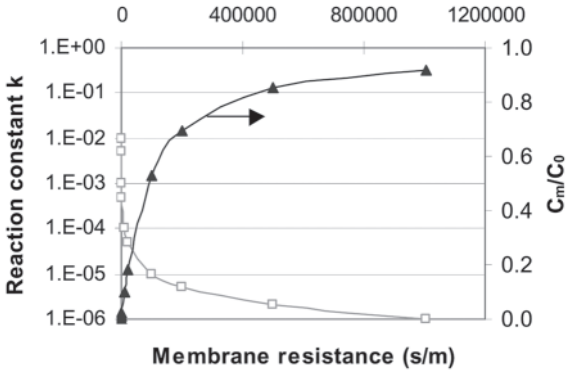

Figure 8. Relationship between the membrane resistance and pseudo-chemical reaction constant and its effect on relative surface concentration at $Re = 450$. The markers represent numerical calculation results.

It is important to realize that this increased surface concentration effect, unlike the situation when surface concentration was increased because of flow regime (see Fig. 9), was actually an indication of decreased separation efficiency.

Figure 9 shows more clearly the effect of membrane resistance on flux and overall resistance. The numerical calculation for different membrane resistance setting showed an almost constant mass transfer coefficient of 1×10^{-5} m/sec in boundary layer when *Re* is 450. The relative flux was calculated as the ratio of the flux calculated with membrane resistance to that calculated without membrane resistance. When membrane resistance increased to about 10,000 sec/m, which is equivalent to the liquid boundary layer resistance in this case, the

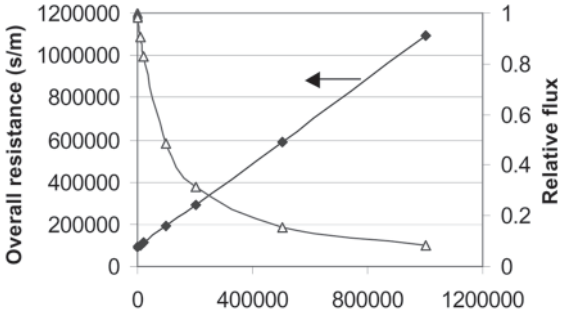

Figure 9. Relationships between the membrane resistance and overall resistance, and the membrane resistance and relative flux at $Re = 450$. The markers represent numerical calculation results.

MARCEL DEKKER, INC.
270 Madison Avenue, New York, New York 10016

flux showed a 50% decrease. After this point the membrane resistance limited the mass transfer. Taking an example of 300 ppm feed solution, the simulated flux result under different flow regimes as a function of membrane resistance is shown in Fig. 10. When membrane resistance is of the order of 1×10^4 sec/m or less, changes in liquid velocity will have a substantial effect on VOC flux. Conversely, in a system with a membrane resistance of 1×10^5 S m or greater, VOC flux will be membrane-limited and a potential performance enhancement would be to find a more efficient membrane rather than improving mass transfer in the boundary layer. The corresponding concentration at the membrane surface in this situation is shown in Fig. 11. As the membrane resistance diminished to a negligible value of 100 sec/m, the surface concentration of the feed stream reached as low as one thousandth of the original concentration. However, it should be noted that while concentration polarization could be regarded as "detrimental" to a PV operation, it is actually an unavoidable phenomenon in any efficient PV operation. The issue is to have a good understanding of the source of mass transfer resistance for better design and evaluation of PV systems.

Mass Transfer Coefficient

The mass transfer coefficients calculated under different feed velocities were shown in Fig. 12 together with the result that was predicted by Leveque's equation. Leveque's equation prediction is smaller than that of the simulation. The discrepancy between the two approaches can be explained by the fact that Leveque's equation is applicable to laminar flows only and could not take into account of the mixing effect at the inlet. The regression of the simulation result in Fig. 12 by a power law series implies that the mass transfer coefficient in the

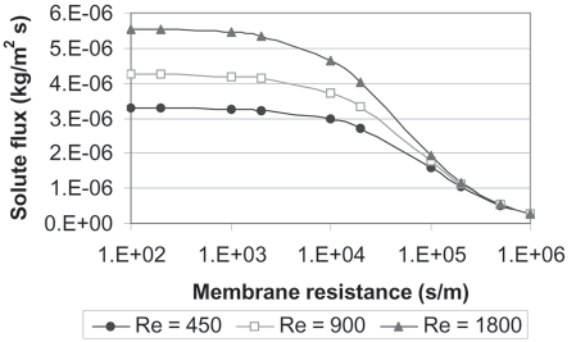

Figure 10. Effect of the membrane resistance on flux under different flow regimes.

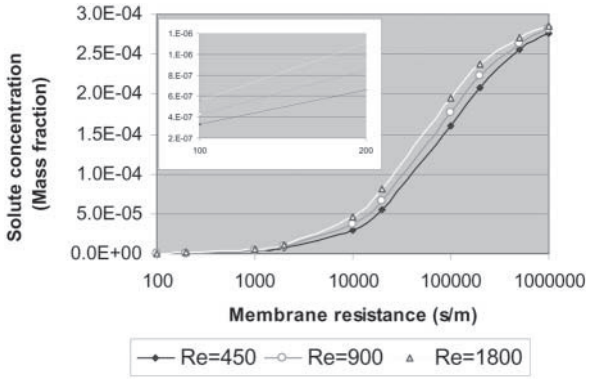

Figure 11. Concentration at membrane surface as a function of membrane resistance under different flow regimes.

membrane channel could be a function of velocity raised to the power of approximate 0.4 instead of 1/3 in the Leveque's equation. As mass transfer is a direct function of membrane module, the conclusion reached in this paper should not be extrapolated to other module without verification although the CFD approach used in this study will apply equally well for other types of PV modules.

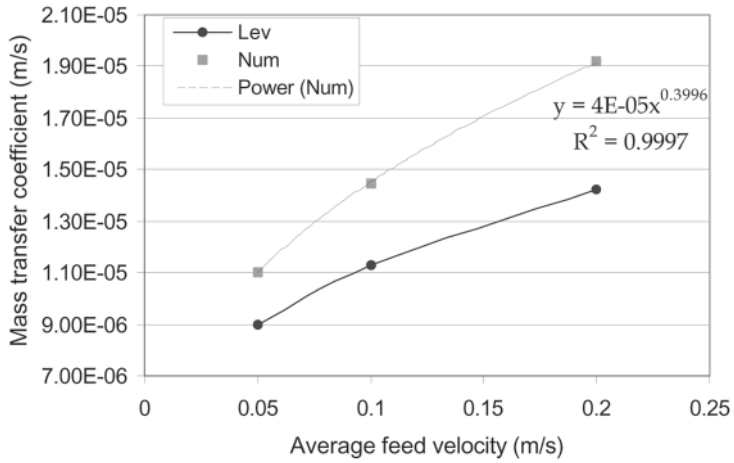

Figure 12. Mass transfer coefficients obtained by the Leveque's equation and the simulation result. The dashed line is regression by a power law expression for simulation results.

As membrane permeabilities for different volatile compounds are not readily available, predicting mass transfer coefficients in the concentration boundary layer becomes particularly important in assessing PV membrane performance in many occasions. Equation (1) has been used for plotting overall mass transfer resistance vs. mass transfer resistance calculated by Eq. (2) in the boundary layer to estimate the membrane resistance by linear extrapolation of the data to obtain the ordinate intercept. This might produce inaccurate estimation if the boundary layer mass transfer coefficient is not correct. Further experimental validation will be required to validate simulation result.

CONCLUSION

A mass transfer model was developed for examining the effect of concentration polarization in a lab-scale PV module. Concentration profile in the membrane channel was found to be a function of position along the membrane surface in the flowing direction. Mass transfer coefficients calculated by this model can take into account the effect of mixing at the inlet of the membrane module channel.

Concentration polarization was examined as a function of both membrane property and flow regime. It was shown to be a coupling phenomenon that ties closely to the PV membrane and the downstream mass transfer resistances. When above-mentioned resistances are small compared to that of the boundary layer on the upstream side, the concentration polarization tends to be severe. Therefore, caution must be exercised when evaluating permeation flux of a PV membrane. The work developed in this paper can be used for evaluating performance of membrane materials in a lab setting. Experimental work will be required for validating the accuracy of numerical results. The tradeoff for using this approach in analyzing mass transfer in PV is the costs involved in both capital investment (computer hardware and software) and computing time. In contrast the traditional approach is more convenient to use in occasions where membrane resistance is large enough to ignore the effect of concentration boundary layer. Future work in this direction will be needed to further quantify the effect of concentration boundary layer on PV separation and scaleup.

NOMENCLATURE

A	proportionality constant
c	solute concentration

MARCEL DEKKER, INC.
270 Madison Avenue, New York, New York 10016

D	diffusion coefficient
d_h	hydraulic diameter
E_a	reaction activation energy
k	mass transfer coefficient
L	length of membrane channel
P	pressure
R	universal gas constant
S	surface area
T	absolute temperature
U	average flow velocity
u	flow velocity in x direction
v	flow velocity in y direction
x, y	coordinates

Greek Symbols

ρ	density of fluid
μ	viscosity of fluid

Superscripts

bl	boundary layer
m	membrane
ov	overall
v	vapor

ACKNOWLEDGMENTS

The research was support financially by U.S. Environmental Protection Agency (CSX 028 QT-OH-00-000532) and New Jersey Agriculture Experiment Station at Rutgers University.

REFERENCES

1. Fleming, H.L.; Slater, C.S. Pervaporation. In *Membrane Handbook*; Ho, W.S.W., Sirkar, K.K., Eds.; Van Nostrand Reinhold Publishers: New York, 1992; 103–159.
2. Aptel, P.; Challard, N.; Cuny, J.; Neel, J. Application of the pervaporation process to separate azeotropic mixtures. J. Membrane Sci. **1976**, *1*, 271–287.

MARCEL DEKKER, INC.
270 Madison Avenue, New York, New York 10016

3. Psaume, J.; Aptel, Ph.; Aurelle, Y.; Mora, J.; Bersillon, J. Pervaporation: importance of concentration polarization in the extraction of trace organics from water. J. Membrane Sci. **1988**, *36*, 373–384.
4. Jiang, J.-S.; Vane, L.; Sikdar, S. Recovery of VOCs from surfactant solutions by pervaporation. J. Membrane Sci. **1997**, *136*, 233–247.
5. Abou-Nemeh, I.; Das, A.; Saraf, A.; Sirkar, K. A composite hollow fiber membrane-based pervaporation process for separation of VOCs from aqueous surfactant solutions. J. Membrane Sci. **1999**, *158*, 187–209.
6. Vane, L.; Hitchens, L.; Alvarez, F.; Giroux, E. Field demonstration of pervaporation for the separation of volatile organic compounds from A surfactant-based soil remediation fluid. J. Hazard. Mater. **2001**, *81*, 141–166.
7. Karlsson, H.; Tragardh, G. Pervaporation of dilute organic-waters mixtures. A literature review on modeling studies and applications to aroma compound recovery. J. Membrane Sci. **1993**, *76*, 121–146.
8. Feng, X.; Huang, R. Concentration polarization in pervaporation separation process. J. Membrane Sci. **1994**, *92*, 201–208.
9. Michaels, A. Effects of feed-side solute polarization on pervaporative stripping of volatile organic solutes from dilute aqueous solution: a generalized analytical treatment. J. Membrane Sci. **1995**, *101*, 117–126.
10. Baker, R.; Wijmans, J.; Athayde, A.; Daniels, R.; Ly, J.; Le, M. The effect of concentration polarization on the separation of volatile organic compounds from water by pervaporation. J. Membrane Sci. **1997**, *137*, 159–172.
11. Dotremont, C.; Van den Ende, S.; Vandommele, H.; Vandecasteele, C. Concentration polarization and other boundary layer effects in the pervaporation of chlorinated hydrocarbons. Desalination **1994**, *95*, 91–113.
12. Binning, R.; Lee, R.; Jennings, J.; Martin, E. Separation of liquid mixtures by permeation. Ind. Eng. Chem. **1961**, *53*, 45–61.
13. Bird, R.; Stewart, W.; Lightfoot, E. *Transport Phenomenon*; John Wiley & Sons: New York, 1960; 62–63.
14. Kolesnikov, I.; Kolesnikov, S.; Vinokurov, V.; Gubkin, I. *Kinetics and Catalysis in Homogeneous and Heterogeneous Systems*; Nova Science Publishers, Inc.: Hauppauge, New York, 2001; 55–57.

Received February 2003
Revised October 2003